

Aerodynamic Analysis of Nonplanar Wings

Mondher Yahyaoui

Borj El Amri Aviation School, Borj El Amri, Tunisia
LASMAP Laboratory, Tunisia Polytechnic School, Tunis, Tunisia.

ABSTRACT

In this work four nonplanar wing configurations were studied using the VLM method: the wing-winglet, the C-wing, the biplane, and the box wing. It has been shown that linear twist, which is more practical in aeronautical construction, is more than adequate when it comes to achieving the higher values of span efficiency factor obtained by a completely optimized, but highly varying, twist distribution along the span camber. It has also been shown that moderate sweep can slightly increase the span efficiency factor, and further reduce vortex drag. But the most important finding is that the wing-winglet configuration and the C-wing, when both have a ratio of winglet/fin bottom chord to wing tip chord equal to 0.5, give the highest reduction in induced drag, clearly outperforming what is known as Prandtl's best wing system. Empirical laws for induced drag ratio all the configurations, including the cases of the wing-winglet and C-wing with a chord ratio of 0.5 were obtained. The biplane and then the box wing configurations have the higher values of lift-to-drag ratio at higher aspect ratios whereas the wing-winglet configuration and C-wing with a chord ratio of 0.5 surpass the biplane and the box wing at lower aspect ratios. Reducing vortex drag can be viewed as more important reducing the overall lift-to-drag ratio of the wing configuration since vortex drag represents a much higher percentage of the overall drag of an aircraft than does the profile drag of the wings alone. From this perspective, the wing-winglet and C-wing with a chord ratio of 0.5 are a better choice than the Prandtl's best wing system.

Keywords: Nonplanar wings, Induced Drag, C-wing, Box Wing, Wing-winglet, Biplane, Lift-to-drag ratio, Span Efficiency Factor.

1. INTRODUCTION

Vortex drag accounts for about 40% of commercial jet transport at cruise conditions and for 80-90% at low speed [1]. The induced drag of plain monoplanes can only be optimized to the extent of having a unit span efficiency factor by achieving an elliptic lift distribution in the spanwise direction. Therefore, in recent years, nonplanar wing configurations have received renewed research interest in view of their potential for attaining much higher values of span efficiency factor and providing major reduction in induced drag.

The idea of nonplanar wings goes back to the 1924 NACA report by Ludwig Prandtl [2] in which it is shown that a box wing, which is basically a biplane connected by end plates, generates less induced drag than other configurations at given lift and span. This configuration was referred to as the best wing system (BWS). According to Prandtl's study, for a height-to-span ratio of 0.2, box wings generate only 68% of the induced drag of a monoplane of equal lift and span. This is equivalent to an overall 12.8% drag reduction in cruise flight (32% of 40%) of a typical jet transport aircraft, and a reduction of 25.6-28.8% at low speeds. These reductions will increase to 16% at cruise speed and 32-36% at low speeds if the fence height-to-span ratio is increased to 0.3.

Adding surface extensions to basic wings to obtain non planar wing configurations such as box wings, C-wings or wing-winglets adds profile drag by increasing wetted area. In addition, for the case of box wings, maintaining equal span and planform area reduces the average chord by half and lowers the wings' Reynolds number, which in turn increases local skin friction. But this is by no means the only drawback associated with box wings. An early investigation into the possibility of integrating box wings into transonic transport is that of Lange *et al* [3]. Their study revealed a number of issues that needed to be solved, in particular the problem of aeroelastic instabilities at a relatively low flutter speed known to be associated with forward swept wings. In [2] the author presents an interesting discussion of the potential for overall aircraft performance improvement associated with nonplanar wing configurations. The main point made is that nonplanar concepts should not be evaluated from an induced drag reduction perspective alone. Other aspects such as the wings structural features may improve overall performance by reducing structural weight.

In spite of the many unsolved issues relating to stability, aeroelastic behavior, and structural efficiency, nonplanar wing configurations have been the subject of numerous aerodynamic studies. Most of these studies are based in the Trefftz

plane and use a discrete vortex lattice method to determine the optimal spanwise lift distribution which yields minimum induced drag [4]-[7]. As shown in Fig. 1, the spanwise distribution of wing and fin twist for minimum induced drag is in general highly varying which makes it of limited practical interest in aircraft construction.

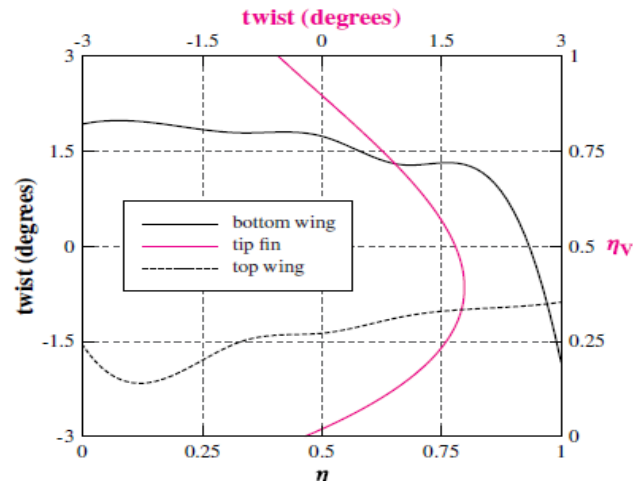


Figure 1. Example of box wings' twist distribution [8].

The objective of the present work is to show that it is possible to achieve the same higher values of span efficiency published in various research papers using only the more practical linear twist for the upper and lower wings and the tip fin. The reference higher values of span efficiency were obtained using a fully optimized yet highly varying twist distribution along the span, making it difficult to apply in aircraft construction.

Four non planar wing configurations were considered (Fig. 2) and the effect of other geometric parameters such as angle of attack, fin height-to-span ratio, sweep, aspect ratio, stagger, and the ratio of the winglet/fin bottom chord to wing tip chord were also studied.



Figure 2. Nonplanar wing considered in this study.

It is also the purpose of this study to make a comparison between the different configurations based on the lowest induced drag criteria and a second based on the maximum overall lift-to-drag ratio for the four configurations. Establishing empirical equations for the induced drag ratio as a function of fin height-to-span ratio is another objective. The investigation is conducted using a cambered VLM program developed by the author [9]. The main results are given in the form of graphical representation of the span efficiency factor and lift-to-drag ratio of the different configurations as functions of various geometric parameters.

2. NUMERICAL METHOD AND VALIDATION

The vortex-lattice method used in this investigation is a singularity method which has been around for many decades and is well documented in the literature [10]. Our VLM MATLAB code accommodates the four configurations subject of this investigation but can also be easily adjusted to include other nonplanar configurations.

While the induced drag coefficient is directly provided by the VLM code, the profile drag coefficient is computed using the equation (Fig. 3):

$$C_{D_p} = \frac{2}{S} \int_0^{s_B} c_d(s) c(s) ds \quad (1)$$

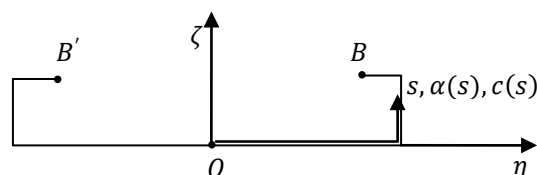


Figure 3. Schematic representation of a typical non planar wing for the computation of profile drag.

Where S is the wing reference area, s is the curvilinear coordinate following the wing span, and $c_d(s)$ is the section profile drag coefficient which depends on the local angle of attack $\alpha(s)$ and the Reynolds number based on the local chord. Numerical values for the local profile drag coefficient are estimated through interpolation using the data curves given in [11] for the chosen wing section.

The key geometric parameters that can be specified are given in Fig. 4. These are:

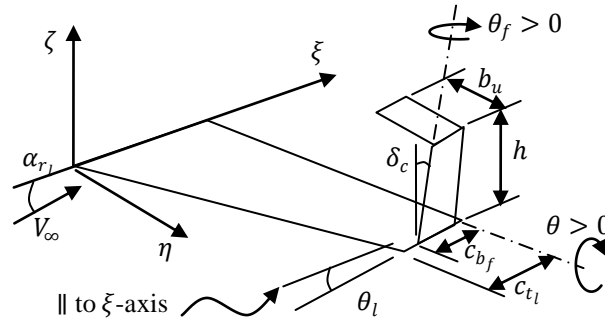


Figure 4. Typical nonplanar wing with key geometric parameters.

- The angle of attack at the root of the lower wing (α_{r_l}).
- The angle of attack at the inner end of the upper wing (α_{i_u}). When a box wing is considered, this angle is the angle at the root of the upper wing.
- The twist angle for lower and upper wings (θ_l, θ_u).
- The twist angle for the winglet/fin (θ_w or θ_f).
- The winglet/fin cant angle (δ_c).
- The height-to-span ratio (h/b).
- The ratio of the upper-wing span to that of the lower wing ($K_b = b_u/b_l$).
- The ratio of the winglet/fin bottom chord to the lower-wing tip chord ($K_c = c_{b_w}/c_{t_l}$).
- Other classical parameters such as aspect ratio (A), sweep (Λ), and taper ratio (λ).

An example of wing configuration treated by our code is shown in Fig. 5.

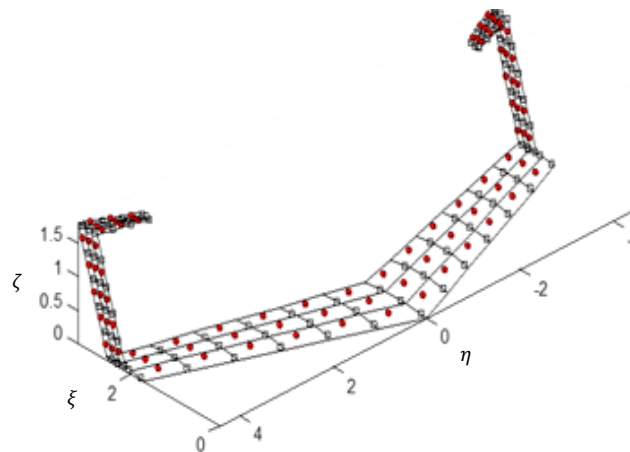


Figure 5. A C-wing modelled by the CVLM code.

Computations using our code will be validated by comparison to published numerical values. The lattice resolution used is 3 rows of panels in the chordwise direction and 25 rows per half span in the spanwise direction. Such a spanwise resolution was sufficient for accuracy to the second decimal place.

A first comparison case consists of a biplane with wings of equal span, an aspect ratio of eight and a height-to-span ratio of 0.5. The value of the span efficiency factor given in [3] is 1.6307. The numerical method used in that work was a vortex-lattice representation of the non-planar wing in the Trefftz plane with an optimum lift distribution in the spanwise direction. The equivalent biplane we considered is of the same geometry except that a linear twist of -3° was applied to both wings. The value given by our code is 1.6392. The relative difference is about 0.5%.

A second case given in the same reference is that of a wing-winglet configuration with an aspect ratio of eight and a height-to-span ratio of 0.1. The value of the span efficiency factor given in [3] is 1.224. The equivalent wing-winglet

combination we considered is of the same geometry ($K_c=1$) except that a linear twist of -2° was applied to the wing and a twist of 0.9° was applied the winglet. The value given by our code is 1.226. The relative difference is about 0.2%.

A third and final comparison is made with values of the span efficiency factor given in [2] as shown in Table 1. **Error! Reference source not found.** The wings have an aspect ratio of 8, a height-to-span ratio of 0.2, and no sweep. Wing twist is equal to -3° for the biplane wings and -2° for the wings of the other three configurations. The winglet/fin twist values are given in the same table. The lift coefficient is equal to 0.5 and the parameter K_c is equal to unity for the wing-winglet and C-wing.

For all four comparison cases, except for the C-wing, the percent difference between our values for the span efficiency factor and the ones from [2] is less than 1%. This is good indication of the accuracy of our computations. For the C-wing, the percent difference is still a reasonable 2%.

Table 1: Comparison of Span Efficiency Factor Values with those from [2]

Geometry	Box wing	C-wing	Wing-winglet	biplane
Reference [2]	1.46	1.45	1.41	1.36
Present work	1.47 ($\theta_f=-0.4^\circ$)	1.42 ($\theta_f=2.5^\circ$)	1.41 ($\theta_w=2.2^\circ$)	1.37
% difference	+0.7	-2	0	+0.7

The span of the upper part of a C-wing was limited to 10% of the main wing span. Beyond this value, the span efficiency factor remains constant while the lift-to-drag ratio keeps on decreasing (Fig. 6) since the induced drag has reached stagnation while the profile and parasite drag continue to increase due to a greater wetted area.

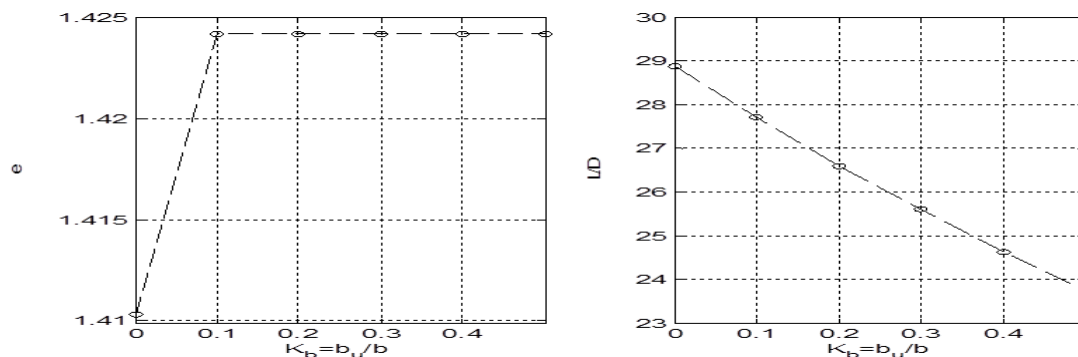


Figure 6. Variation of e and L/D with the ratio K_b for a C-wing with $A=8$, $h/b=0.2$, $\Lambda=0$, $\lambda=1$, $C_L=0.5$, $K_c=1$, and θ_f optimized for each K_b .

3. RESULTS AND DISCUSSION

Unless otherwise specified, the aspect ratio of the different wing configurations is equal to 8 and the lift coefficient is equal to 0.5. Such a value is representative of cruise flight. The winglet/fin twist angle is optimized based on the highest values of span efficiency factor and not on that of the highest L/D ratio. This was done manually by running the code for different values of this $\theta_{w/f}$. An example of finding the “optimal” fin twist angle is shown in Fig. 7 for the C-wing.

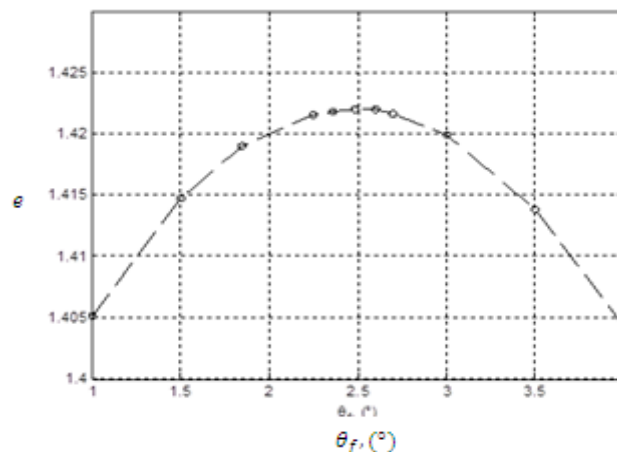


Figure 7. An illustrative example of finding fin twist angle given for an unswept C-wing with $A=8$, $\lambda=1$, $\theta=-2^\circ$, $h/b=0.2$, $K_c=1$, $K_b=0.1$, and $C_L=0.5$

The equivalent planar wing used for comparison is assumed to have the same aspect ratio, operate at the same lift coefficient and have an elliptic lift distribution in the spanwise direction so that its span efficiency factor is equal to unity.

The induced drag coefficient is given by the equation:

$$C_{Di} = \frac{C_L^2}{\pi e A} \quad (2)$$

Therefore the ratio of the induced drag coefficient of any configuration to that of the reference planar wing is:

$$r = D_i/D_{i_r} = C_{Di}/C_{Di_r} = e_r/e$$

For $e_r = 1$ we get:

$$r = 1/e \quad (3)$$

All the computations were conducted in the incompressible regime and, since airfoil camber has basically no influence on the results, the symmetrical NACA 0012 was used for the main wing, vertical extension and upper wing. The twist of the upper wing of the box wing configuration was set equal to that of the lower wing. But no twist was given to the upper portion of the C-wing.

A. Effect of Wing Twist

The effect of wing twist on the span efficiency factor is shown in Fig. 8. From a purely aerodynamic efficiency perspective, this parameter will be chosen as to maximize the value of e . In practice, higher values may be chosen in order to obtain a better wing stall behavior and avoid spin departure.

Throughout this study, unless otherwise specified, the following values for wing twist are retained:

- $\theta = -2^\circ$ for the wing of the wing-winglet system, the C-wing and both wings of the box wing.
- $\theta = -3^\circ$ for both wings of the biplane and for the equivalent planar wing.

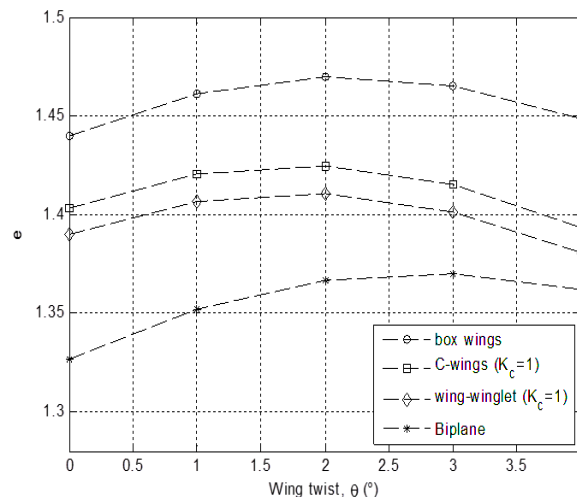


Figure 8. Effect of wing twist (θ) on e for $A=8$, $h/b=0.2$, $\Lambda=0$, $\lambda=1$, $C_L=0.5$, and optimal $\theta_{w/t}$ for each θ .

B. Effect of Lift Coefficient

The lift coefficient has an effect on the span efficiency factor that is different from that on the lift-to-drag ratio. As indicated on Fig. 9-(a), the latter reaches a maximum at a lift coefficient of about 0.4 to 0.5 for all the configurations considered, including the cases of the wing-winglet configuration and the C-wing with $K_c=0.5$.

The span efficiency factor on the other hand exhibits a different behavior for the wing-winglet configuration and for the C-wing when $K_c=0.5$. When the winglet/fin twist angle is optimized for $C_L=0.5$, the efficiency factor reaches a maximum at around this value of the lift coefficient for the four basic configurations (Fig. 9-(b)). The difference between the minimum and maximum value of e is rather small: it varies between 0.5% for the box wing to 2% for the C-wing with $K_c=1$.

But, for the wing-winglet configuration and for the C-wing with $K_c=0.5$, this factor keeps on increasing with lift coefficient and the difference between the values of e at $C_L=0.5$ and at $C_L=0.8$ is 1.4% for the wing-winglet configuration and 1.3% for the C-wing. This is a rather interesting result since induced drag is higher at low speeds, where the lift coefficient is high.

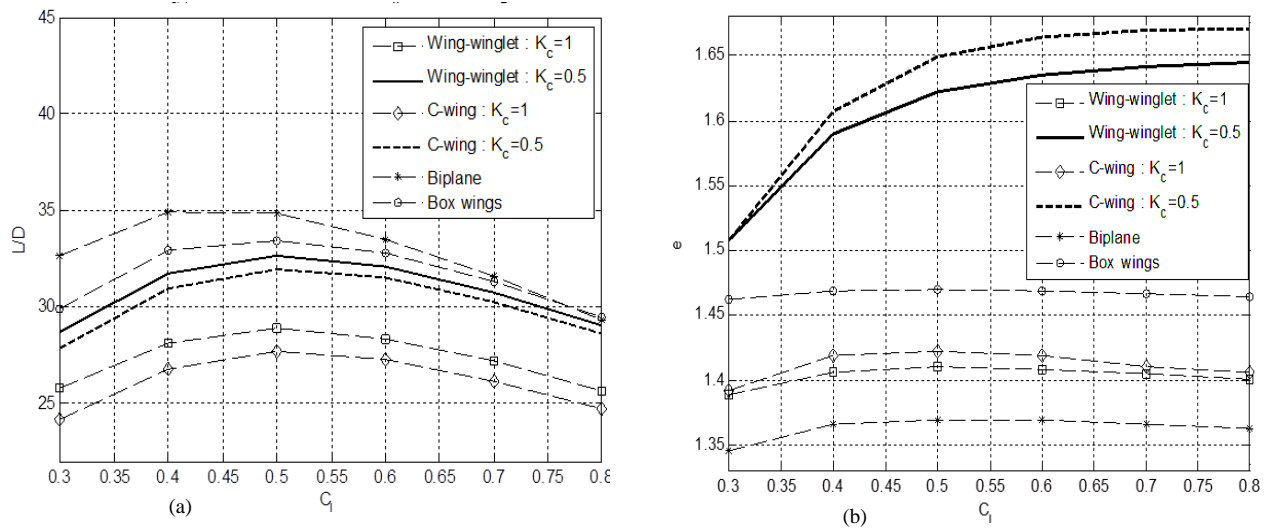


Figure 9. Variation of e and L/D with C_L for $A=8$, $h/b=0.2$, $\Lambda=0$, $\lambda=1$, and $\theta_{w/f}$ optimized for $C_L = 0.5$

In order to further assess the combined effect of lift coefficient and winglet/fin twist when K_c is equal to 0.5, the wing-winglet configuration is considered and the winglet twist is optimized for two different values of C_L (0.5 and 0.8). The results for the C-wing generally follow the same overall pattern.

As shown on Fig. 10 (a), the maximum lift-to-drag ratio is reached at a C_L value of about 0.5 even when the winglet twist angle is optimized for $C_L=0.8$ although in this case the value of L/D at $C_L=0.5$ decreases by 1.6%. The overall variation of the span efficiency factor remains the same when θ_w is optimized for $C_L=0.8$ instead of $C_L=0.5$, i.e. it is strictly increasing (Fig. 10-(b)). However, at the latter value of C_L , e decreases by 2.6% while an increase of 1% is noted for $C_L=0.8$.

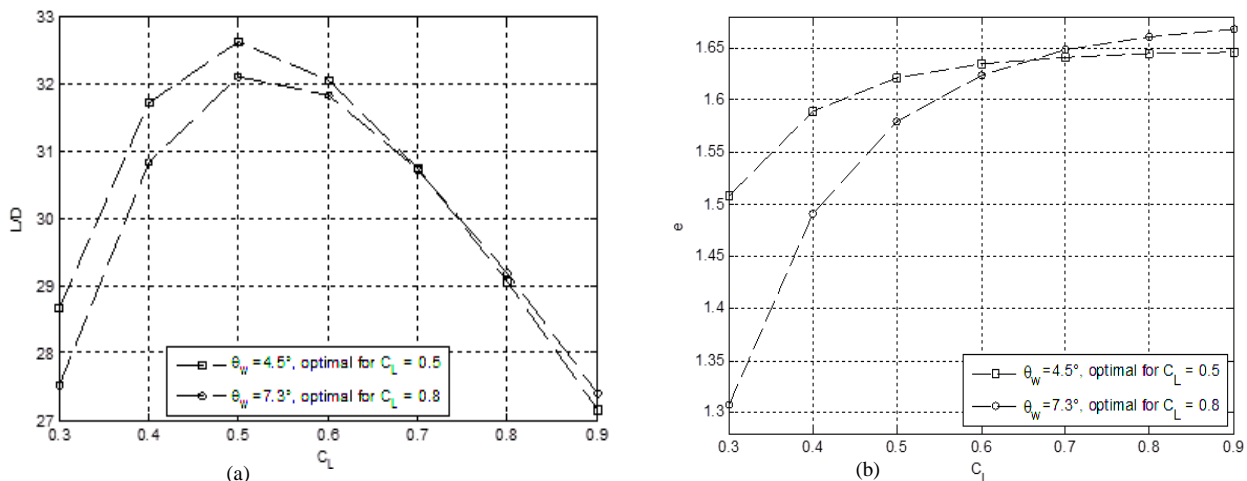


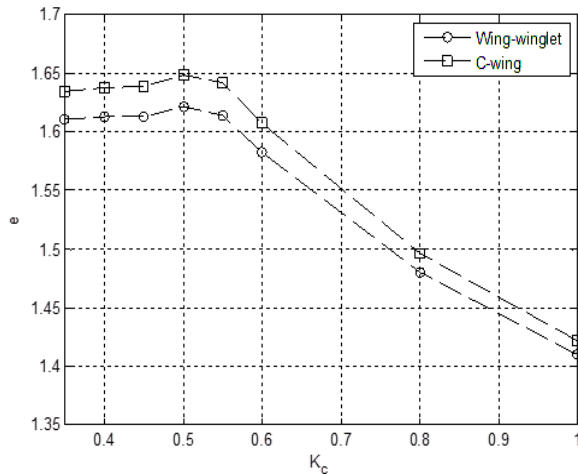
Figure 10. Variation of e and L/D with C_L for a wing-winglet with $A=8$, $h/b=0.2$, $\Lambda=0$, $\lambda=1$, $K_c=0.5$, and $\theta_{w/f}$ optimized for two values of C_L

C. Effect of Chord Ratio

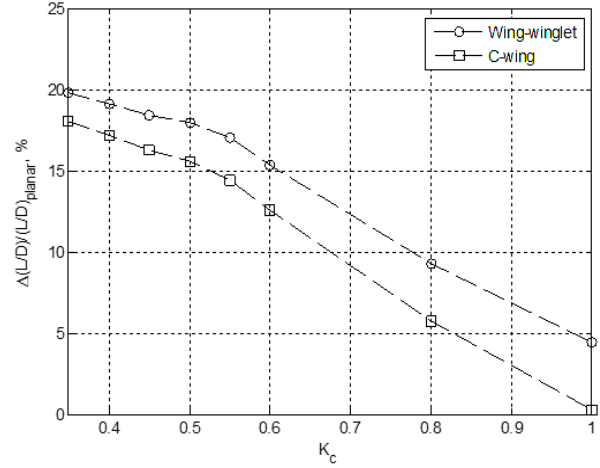
The chord ratio K_c is a key parameter affecting the wing-winglet configuration and the C-wing. As seen on Fig. 11, this parameter has a major effect of both the span efficiency and the overall wing aerodynamic efficiency as measured by the lift-to-drag ratio. When K_c is reduced from 1 to 0.5, the span efficiency increases from 1.42 to 1.65 for the C-wing, a 16% increase. As for the wing-winglet configuration, this factor increases from 1.41 to 1.62 which is an increase of about 15%.

The effect on the lift-to-drag ratio is similar. When compared to the equivalent planar wing, the wing-winglet with $K_c=0.5$ generates a lift-to-drag ratio which is greater by 18% instead of 4% for $K_c=1$. For the C-wing, the gain is 15.6% for $K_c=0.5$ and practically no gain for $K_c=1$.

The equivalent planar wing has a -3° twist, the same aspect ratio of 8 and generates the same lift coefficient of 0.5. Its lift-to-drag ratio is equal to 27.66. Higher gains in the lift-to-drag ratio can be achieved if K_c is reduced below 0.5 but too much reduction in the vertical extension chord may compromise the structural integrity of the wing configuration.



(a) Variation of the span efficiency factor with K_c



(b) Increase in L/D ratio compared to the equivalent planar wing

Figure 11. Effect of K_c on the C-wing and wing-winglet for $A=8$, $\Lambda=0$, $\lambda=1$, $\theta=-2^\circ$, $h/b=0.2$, $C_L=0.5$, and $\theta_{w/f}$ optimized for each K_c .

D. Effect of Sweep

When a 20° sweep at the quarter chord is applied to wings and end fins alike, the span efficiency factor e increases from (Fig. 12-(a)):

- 1.41 to 1.44 for a wing-winglet with $K_c=1$.
- 1.62 to 1.65 for a wing-winglet with $K_c=0.5$.
- 1.42 to 1.46 for a C-wing with $K_c=1$.
- 1.65 to 1.68 for a C-wing with $K_c=0.5$.
- 1.37 to 1.41 for a biplane with a positive stagger of two chord lengths.

The e value for a box wing increases from 1.47 to 1.48 for a sweep of 10° .

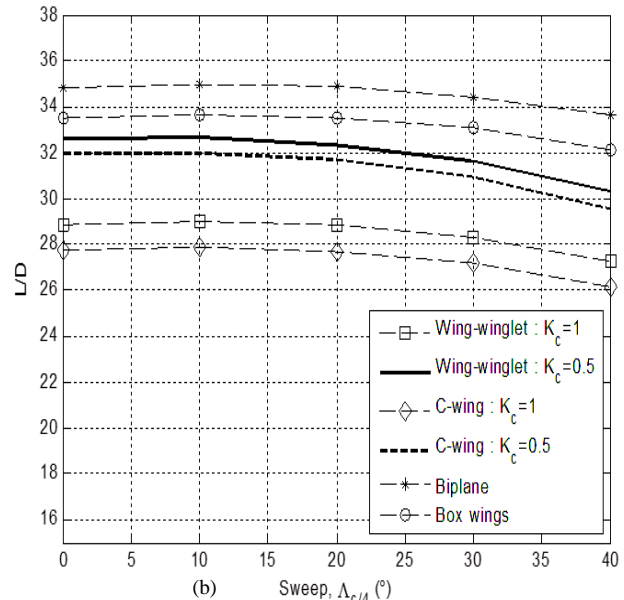
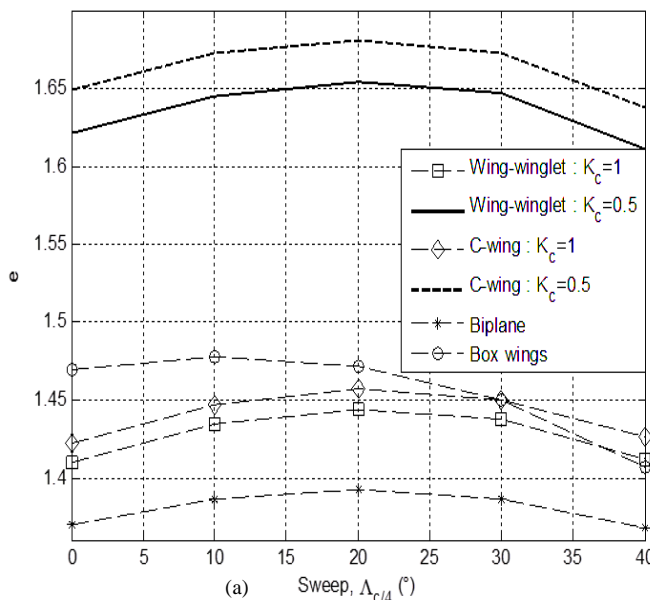


Figure 12. Effect of sweep on e and L/D for $A=8$, $\lambda=1$, $h/b=0.2$, $C_L=0.5$, and $\theta_{w/f}$ optimized for each A

The wing-winglet configuration and the C-wing both with a K_c ratio of 0.5 offer the highest values of span efficiency. If the reference value of e for the box wing is taken as 1.46 [2], then the unswept wing-winglet configuration with $K_c=0.5$ outperforms the Prandtl's best wing system (BWS) by 11% while the C-wing with equal K_c has an e value that is 13% higher. The gain will be slightly better if a 20° sweep is given to both configurations. However, if we were to look at the overall lift-to-drag ratio of the four configurations (Fig. 12-(b)), then it is clear that, at this value of aspect ratio, the biplane configuration gives the highest value, followed by the box wing.

E. Effect of Aspect Ratio

As for planar wings, the span efficiency factor of non planar configurations decreases with aspect ratio (Fig. 13) and the decrease is far more remarkable for the wing-winglet and C-wing with $K_c=0.5$. However, the effective aspect ratio (eA) increases linearly for all the configurations which explains the decrease of the induced drag coefficient, the latter being inversely proportional to the effective aspect ratio.

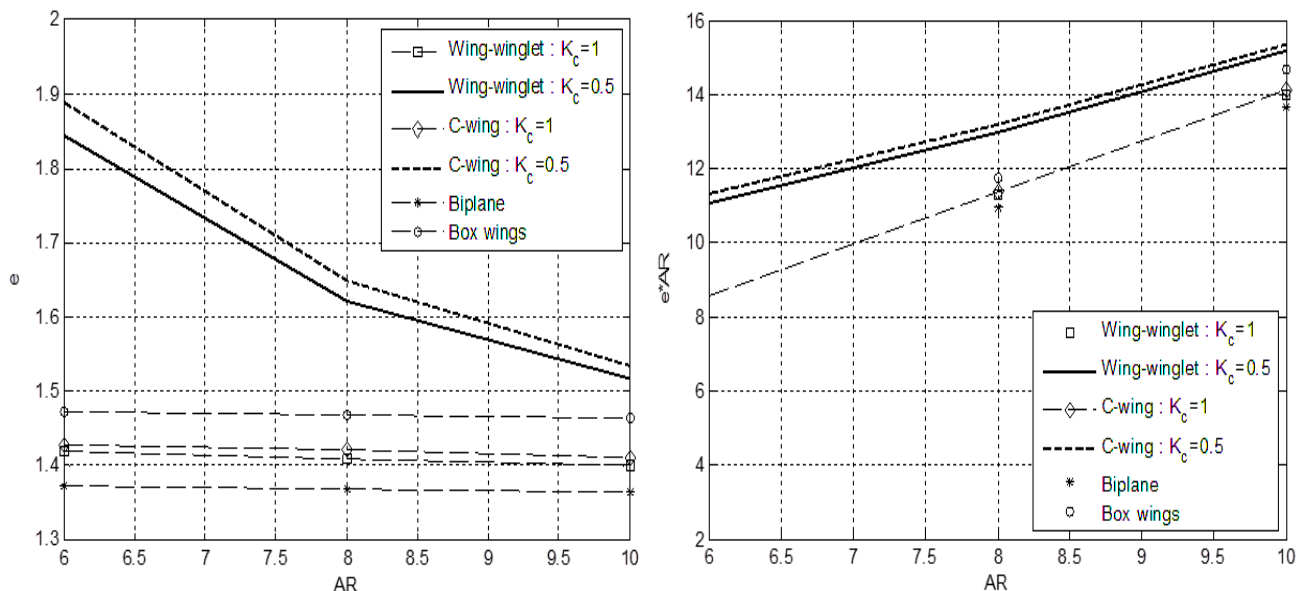


Figure 13. Variation of e and the product “ eA ” with aspect ratio for $\Lambda=0$, $\lambda=1$, $h/b=0.2$, $C_L=0.5$, and $\theta_{w/t}$ optimized for each A

At an aspect ratio of 6 (Fig. 14), the wing-winglet configuration with $K_c=0.5$ gives the highest value of lift-to-drag ratio: 1.4% higher than the C-wing with $K_c=0.5$, 1.8% higher than the biplane, and 4.4% higher than the box wing. But at higher aspect ratios, the biplane will have the highest ratio of lift-to-drag, followed by the box wing, then the wing-winglet configuration with $K_c=0.5$. The gain in aerodynamic performance relative to the equivalent planar wing of equal aspect ratio decreases with aspect ratio for all configurations. In particular, at an aspect ratio higher than eight, the C-wing with $K_c=1$ will have an L/D ratio less than that of its equivalent planar wing.

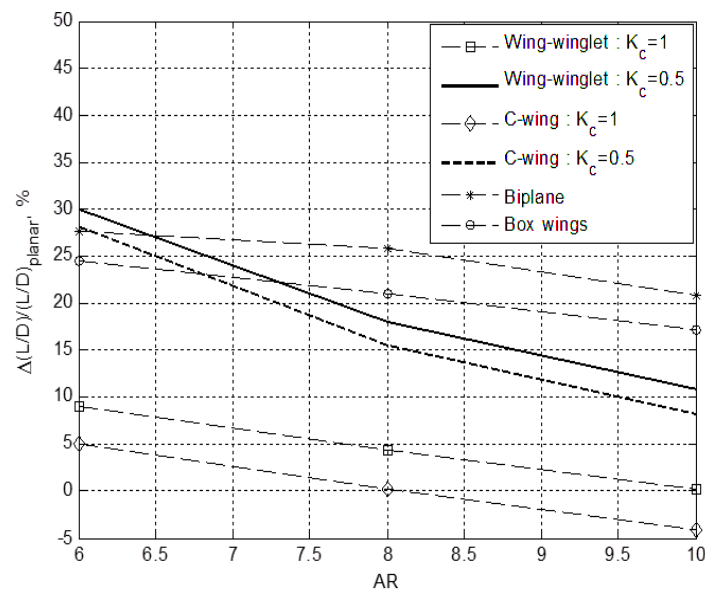


Figure 14. Change in L/D relative to the equivalent planar wing as a function of aspect ratio: $\Lambda=0$, $\lambda=1$, $h/b=0.2$, $C_L=0.5$, and $\theta_{w/f}$ optimized for each A

A summary of the main results for an aspect ratio of 8 and $h/b=0.2$ is given in Table 2 where the percent increase in the L/D ratio with respect the equivalent planar wing is given. As noted previously, the biplane and box wing have the better values of L/D for this higher value of aspect ratio.

Table 2: Summary of results for $A=8$, $h/b=0.2$, and $C_L=0.5$

Case	e	L/D	Increase in L/D (%)
Wing-winglet ($K_c = 1$, $\Lambda=0$)	1.41	28.28	2.2
Wing-winglet ($K_c = 0.5$, $\Lambda=0$)	1.62	32.63	18.0
Wing-winglet ($K_c = 0.5$, $\Lambda=20^\circ$)	1.65	32.36	16.6
C-wing ($K_c = 0.5$, $\Lambda=20^\circ$)	1.42	27.73	0.3
C-wing ($K_c = 0.5$, $\Lambda=0$)	1.65	31.97	15.6
C-wing ($K_c = 0.5$, $\Lambda=20^\circ$)	1.68	31.68	14.5
Box wing ($\Lambda=10^\circ$)	1.48	33.63	21.6
Biplane ($\Lambda=20^\circ$, $St = 2c$)	1.41	34.98	25.9

The most noteworthy values of span efficiency factor are given on Fig. 15. When compared to a monoplane of equal aspect ratio and lift coefficient and having a unit span efficiency factor, an unswept C-wing with a height-to-span ratio of 0.2, $K_b=0.1$ and $K_c=0.5$ has a span efficiency factor equal to 1.65 and therefore gives 60.6% of the induced drag. A similar wing but with a 20° positive sweep has a span efficiency factor equal to 1.68 only 59.5% of the induced drag of the optimized planar wing. Similarly, an unswept wing-winglet with equal values of h/b and K_c has $e=1.62$ and generates 61.7% of the induced drag and the same configuration with 20° sweep has $e=1.65$ and generates 60.6%.



Figure 15. Highest values for span efficiency factor obtained for $A=8$, $\Lambda=0$, $\lambda=1$, $h/b=0.2$, and $C_L=0.5$

F. Effect of Height Ratio

The effect of the ratio of winglet/fin height to wing span is presented in terms of the ratio of the induced drag of the non planar configuration to that of the reference planar wing. The results given in Fig. 16-(a) show that, for values of height-to-span ratio of practical interest (0.2 or less), our results for the box wing configuration identically duplicate what is known as the Prandtl's BWS. Figure 16-(b) shows that, once again, the wing-winglet and the C-wing configurations with a chord ratio $K_c=0.5$ have the lowest induced drag. They both outperform the Prandtl's BWS for values of h/b less than 0.42.

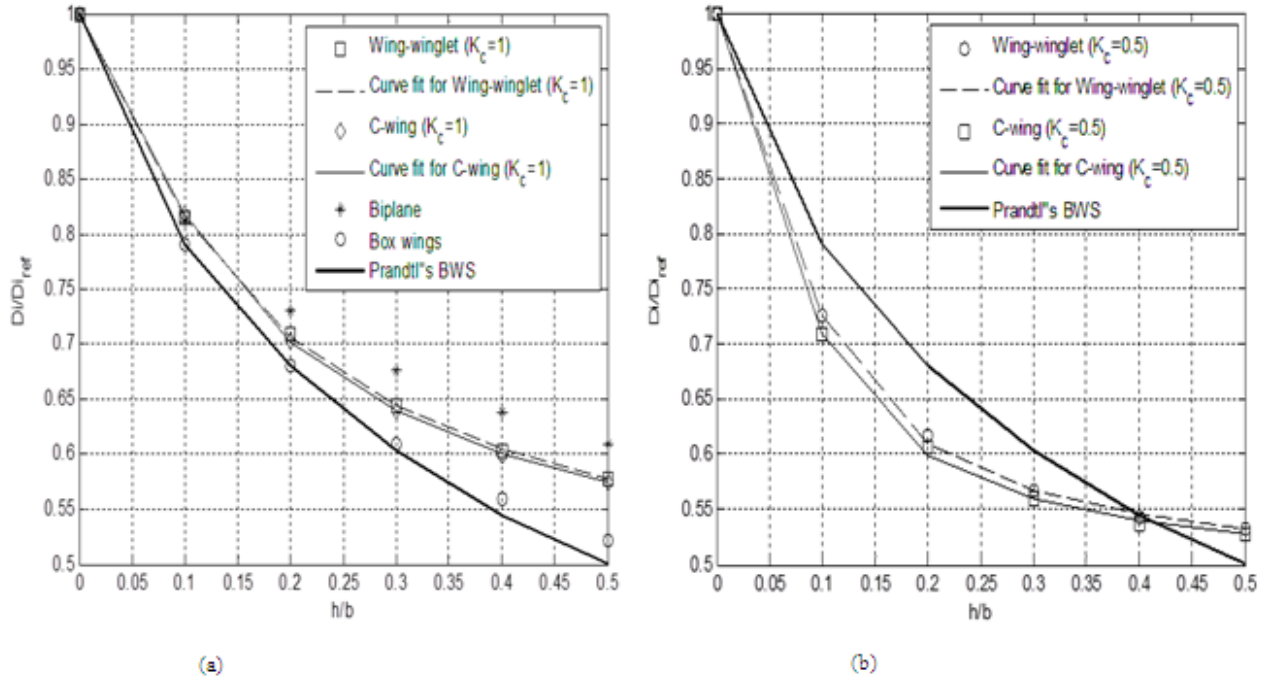


Figure 16. Effect of height-to-span ratio on the induced drag ratio for $A=8$, $\Lambda=0$, $\lambda=1$, $h/b=0.2$, $C_L=0.5$, and $\theta_{w/f}$ optimized for each h/b .

As shown in Fig. 17-(a), the C-wing configuration with $K_c=0.5$ gives a 10.3% less induced drag than the Prandtl's BWS for $h/b=0.1$ and 10.9% for $h/b=0.2$. Similarly, the wing-winglet configuration with $K_c=0.5$ gives 8.3% less induced drag for $h/b=0.1$ and 9.4% for $h/b=0.2$. For values of h/b higher than 0.42 or so, the Prandtl's BWS gives the least induced drag.

Looking at Fig. 17-(b), it is clear that, for an aspect ratio of 8, the biplane gives the highest values of the lift-to-drag ratio for all height-to-span ratios. When compared to the equivalent planar wing and for $h/b=0.2$, the biplane improves the L/D ratio by 25.9%, the box wing by 21.1%, the wing-winglet with $K_c=0.5$ by 18%, and the C-wing with $K_c=0.5$ by 15.6%. While the wing-winglet with $K_c=1$ improves the L/D ratio by a modest 4.4%, the C-wing with $K_c=1$ has practically no interest at all.

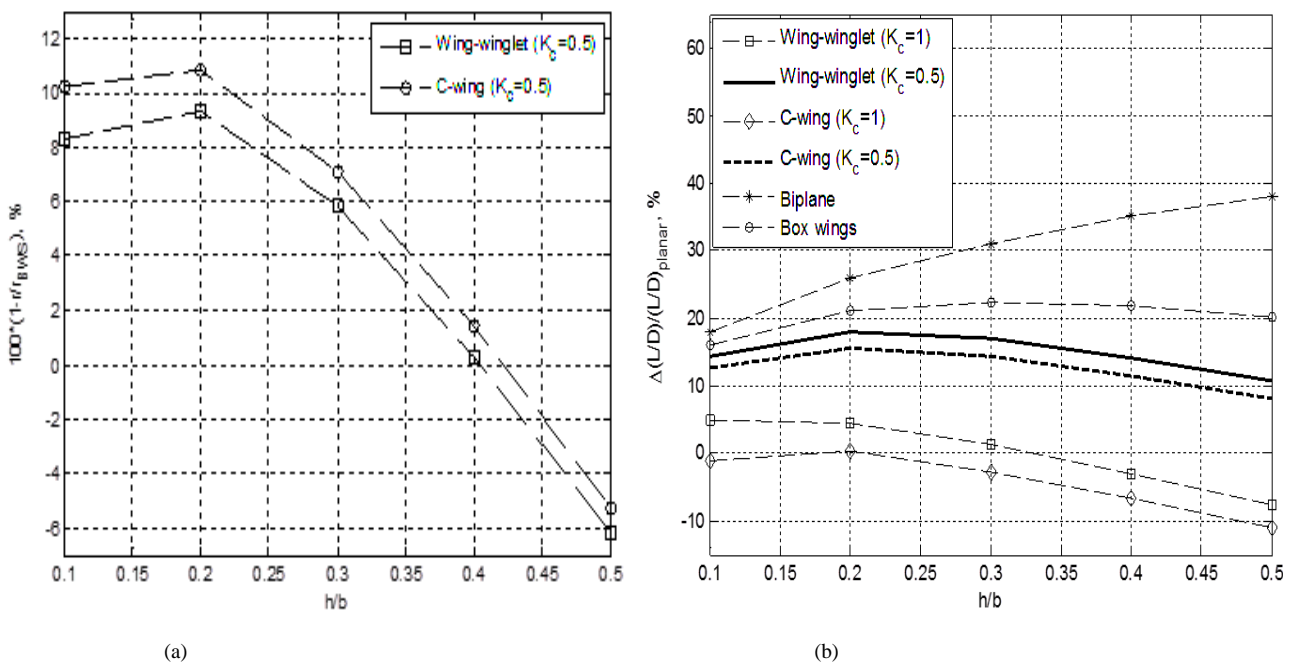


Figure 17. Nonplanar configurations with $A=8$, $\Lambda=0$, $\lambda=1$, $C_L=0.5$, and $\theta_{w/f}$ optimized for each h/b : (a) Change in the induced drag ratio compared to Prandtl's BWS for the C-wing and wing-winglet when $K_c = 0.5$ (b) Change in L/D ratio relative to the equivalent planar wing for all six configurations.

G. Empirical Laws for the Induced Drag Ratio

The empirical law for the induced drag ratio is assumed as in [1] to be in the form:

$$r = \frac{1 + c_1 x}{c_2 + c_3 x} \quad (4)$$

where x is the height-to-span ratio and r is the induced drag ratio, defined previously.

The three unknown constants are determined by solving a linear system of three equations in these constants, obtained by requiring that the curve representing the induced drag ratio go through three points of our choice. It is found that choosing $x_1 = 0, x_2 = 0.2$ and $x_3 = 0.5$ as abscissa of these points yields curve fits which fairly accurately match the discrete data (Fig. 16). The three unknown constants are thereby solutions to the following system:

$$\begin{pmatrix} x_1 & -r_1 & -r_1 x_1 \\ x_2 & -r_2 & -r_2 x_2 \\ x_3 & -r_3 & -r_3 x_3 \end{pmatrix} \begin{bmatrix} c_1 \\ c_2 \\ c_3 \end{bmatrix} = \begin{bmatrix} -1 \\ -1 \\ -1 \end{bmatrix} \quad (5)$$

Applying this approach to the different configurations considered we get:

- **Wing-winglet with $K_c = 1$**

$$r_{ww} = \frac{1 + 2.6045 h/b}{0.9353 + 6.1002 h/b}, \quad \lim_{h/b \rightarrow \infty} r_{ww} = 0.4269 \quad (6)$$

- **Wing-winglet with $K_c = 0.5$**

$$r_{ww} = \frac{1 + 13.1996 h/b}{0.4274 + 27.7113 h/b}, \quad \lim_{h/b \rightarrow \infty} r_{ww} = 0.4763 \quad (7)$$

- **C-wing with $K_c = 1$**

$$r_{cw} = \frac{1 + 3.0383 h/b}{0.8961 + 6.9795 h/b}, \quad \lim_{h/b \rightarrow \infty} r_{cw} = 0.4353 \quad (8)$$

- **C-wing with $K_c = 0.5$**

$$r_{cw} = \frac{1 + 15.3563 h/b}{0.3503 + 32.2139 h/b}, \quad \lim_{h/b \rightarrow \infty} r_{cw} = 0.4767 \quad (9)$$

- **Biplane**

Present work:

$$r_{bp} = \frac{1 + 1.5477 h/b}{1.0513 + 3.7129 h/b}, \quad \lim_{h/b \rightarrow \infty} r_{bp} = 0.4169 \quad (10)$$

Prandtl's result:

$$r_{bp} = \frac{1 + 1.4829 h/b}{1.0500 + 3.6098 h/b}, \quad \lim_{h/b \rightarrow \infty} r_{bp} = 0.4108 \quad (11)$$

The relative difference between our limit value and that given by Prandtl's equation is only 1.5%.

- **Box wing**

Present study:

$$r_{bw} = \frac{1 + 1.0303 h/b}{1.0202 + 3.7586 h/b}, \quad \lim_{h/b \rightarrow \infty} r_{bw} = 0.2741 \quad (12)$$

Prandtl's equation was:

$$r_{bw} = \frac{1 + 0.45 h/b}{1.04 + 2.81 h/b}, \quad \lim_{h/b \rightarrow \infty} r_{bw} = 0.16 \quad (13)$$

While a more recent study [12] gave the following equation:

$$r_{bw} = \frac{1 + 2.18 h/b}{1 + 5.04 h/b}, \quad \lim_{h/b \rightarrow \infty} r_{bw} = 0.43 \quad (14)$$

Our result for the limit value is comprised between the latter value and that of Prandtl.

An exact solution to the Prandtl's problem was first published in [13] and a sketchy graph based on that solution is given in [14]. This graph is reproduced in Fig. 18 as to make a visual comparison of our results for the induced drag ratio of the box wing as a function of h/b to those from this reference and from Prandtl's BWS solution. It is seen that, in the practical range of values of h/b (less than 0.2), our results identically reproduce those of Prandtl while at higher values closer agreement with the exact solution of [13] is shown.

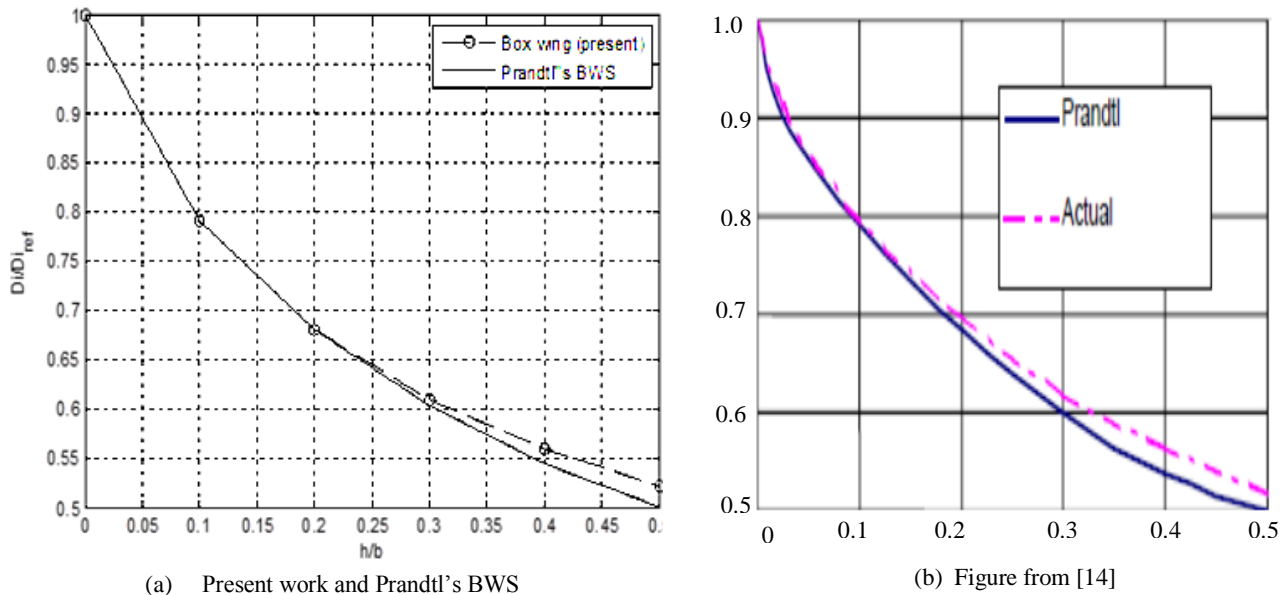


Figure 18. Comparison of the ratio Di/D_r from the present work and from [13] to Prandtl's BWS for $A=8$, $\Lambda=0$, $\lambda=$, $C_L=0.5$, and θ_f optimized for each h/b

CONCLUSION

In this work four nonplanar wing configurations were studied using the vortex-lattice method: the wing-winglet, the C-wing, the biplane, and the box wing. It has been shown that linear twist, which is more practical in aeronautical construction, is more than adequate when it comes to achieving the higher values of span efficiency factor obtained by a completely optimized twist distribution along the span camber, the latter being in general highly varying and thus not very practical. It has also been shown that moderate sweep can slightly increase the span efficiency factor and further reduce vortex drag.

But the most important finding of this investigation is that the wing-winglet configuration and the C-wing, when both have a ratio of winglet/fin bottom chord to wing tip chord equal to 0.5, give the highest reduction in induced drag, clearly outperforming what is known as Prandtl's best wing system by providing a further reduction of induced drag of about 10% for a height-to-span ratio of 0.2. This result is in agreement with the geometric shape of the Whitcomb winglet which in general occupies an aft portion of the wing tip. But it also seems to be in disagreement with what is commonly recognized that the span efficiency is independent of the longitudinal position of the vertical surface extension. Reducing the winglet or fin chord and placing it on the aft half of the wing tip reduces all forms of aerodynamic interference between winglet and wing, both at high angle of attack and in the transonic regime.

When assessed from the perspective of the overall lift-to-drag ratio, the biplane and then the box wing configuration have the highest values except at the lower values of aspect ratio. At an aspect ratio of 6.5 or less, the wing-winglet configuration with $K_c=0.5$ has the highest value of L/D . At an aspect ratio of about 6 or less, even the C-wing with $K_c=0.5$ begins to surpass the biplane and the box wing.

Reduction in vortex drag can be viewed as more important than that in the overall lift-to-drag ratio of the wing configuration since vortex drag takes a much higher percentage of the overall drag than does the profile drag of the wings alone. As mentioned at the beginning of this article, the vortex drag represents as much as 90% of the total drag at low speed flight and as much as 40% in cruise flight, for jet transports at least. From this perspective, the C-wing and the wing-winglet configuration with their bottom chord reduced to 50% of the wing tip chord outperform all the other configurations studied by a considerable margin, including the so called Prandtl's best wing system.

REFERENCES

- [1]. L. Prandtl "Induced drag of multiplanes", NACA TN 182, 1924.
- [2]. I. Kroo, "Nonplanar wing concepts for increased aircraft efficiency". Innovative configurations and advanced concepts for future civil aircraft, Von Karman Institute, Brussels, Belgium, 2005.
- [3]. R. H. Lange, J. F. Cahill, E.S. Bradley, R. R. Eudaily, C. M. Jenness, and D. G. MacWilkinson, "Feasibility Study of the Transonic Biplane Concept for Transport Aircraft Application," NASA CR-132462, 1974.
- [4]. J. A. Blackwell, "Numerical method to calculate the induced drag or optimum loading for arbitrary non-planar aircraft," NASA SP-405, 1976.

- [5]. J. E. Lamar, "A vortex-lattice method for the mean camber shapes of trimmed non coplanar planforms with minimum induced drag," NACA TN D-8090, 1976.
- [6]. J. Kuhlman and T. Ku, "Numerical optimization techniques for bound circulation distribution for minimum induced drag of nonplanar wings: computer program documentation," NASA CR-3458, 1982.
- [7]. Kroo, I., "A general Approach to Multiple Lifting Surface Design and Analysis", AIAA paper 84-2507, Oct. 2004.
- [8]. H. Gagnon and D. W. Zingg, "Aerodynamic Optimization Trade Study of a Box-Wing Aircraft Configuration," AIAA.
- [9]. M. Yahyaoui, "Generalized vortex lattice method for predicting characteristics of wings with flap and aileron deflection", Int. Journal. of Mechanical, Aerospace, Industrial, and Mechatronics Engineering, 2014, Vol. 8.
- [10]. J. J. Bertin and M. L. Smith, *Aerodynamics for engineers*, 3rd Ed, Prentice Hall, 1998.
- [11]. I. H. Abbot and A. E. Von Doenhoff, *Theory of wing sections*, Dover, 1959.
- [12]. E. Rizzo, *Optimization Methods applied to the Preliminary design of Innovative, Non Conventional Aircraft Configurations*, Edizioni ETS, Pisa, 2007, ISBN 978-884672458-8.
- [13]. A. Frediani and G. Montanari: "An exact solution to the Prandtl's Problem". In: *Variational Analysis and Aerospace Engineering*, Springer, 2009, pp 183-211, ISBN 978-0-387-95856-9.
- [14]. A. Frediani: "The Prandtl Wing". In: *VAN KARMON INSTITUTE FOR FLUID DYNAMICS, VKI Lecture series : Innovative Configurations and Advanced Concepts fo Future Civil Transport Aircraft*. Von Karmon Institute for Fluid Dynamics, 2005
- [15]. H; H. Heyson, G. D. Riebe, and C. L. Fulton, "Theoretical Parametric Study of the Relative Advantages of Winglets and Wing-Tip Extensions, NASA Technical Paper 1020, 1977.